Journal of Nepal Geological Society, 2001, Vol. 23, pp. 91–98

Soil and rock strength parameters of the Shiraidake Landslide, Japan

Robert Jelinek, Prem Prasad Paudel, and Hiroshi Omura
Laboratory of Forest Conservation, Department of Forest and Forest Products, Faculty of Agriculture, Kyushu University, Higashi-ku, Hakozaki 6-10-1, Fukuoka 812-8581, Japan

ABSTRACT

The Shiraidake area of northwest Kyushu has an extensive distribution of landslides. A series of undrained triaxial tests and unconfined compression tests were carried out to investigate the variation of strength properties in a selected borehole from the Shiraidake Landslide. It is a translational landslide (called the *Hokusho*-type in Japan) and is composed of the Early Tertiary and Quaternary sedimentary rocks that are prone to rapid weathering. Core rock samples and recompacted soil samples were used for the study. The results provided the fundamental characteristics of soil and rock under the triaxial and uniaxial tests, and indicated that the undrained behaviour of tested soils generally depends on the pre-shear consolidation pressure and dry density. In addition, the type of material used and the tests performed are important factors that influence the soil and rock strength.

INTRODUCTION

Landslides due to the geological conditions, steep terrain, and heavy rains cause economic loss and sometimes even the loss of human lives in Japan. The study area (Fig. 1) is located about 1 km E of the Matsuura City, Nagasaki Prefecture, northwest Kyushu (33° 20′ N, 129° 44′ E). The landslide is developed on the western slope of Mt. Shiraidake (358.8 m), on the right bank of the Tsukinokawa River. The surrounding area is moderately steep and has an extensive distribution of landslides.

Under the influence of gravity, due to tectonic stresses, seismic activity etc, the material composing any slope has a natural tendency to slide. On the other hand, the material also possesses the shearing resistance against sliding. Instability occurs when the shearing resistance is not enough to overcome the forces tending to cause movement along any surface within a slope (Chowdhury 1978).

According to Fujita (1999), most of the landslides classified in the slow-type are found on soft and fine clastic rocks. He pointed out that such rocks show tendencies to form slip surfaces, because of abundant clay minerals, particularly, those containing montmorillonite.

To understand the landslide phenomena, it is essential to have knowledge about soil and rock properties, stress–strain of mass, and mechanism of movement. Other types of information such as the groundwater conditions defined by the water table, pore pressure, geological and morphological conditions, and type and frequency of processes are also essential.

The principal parameter controlling sliding of soil and rock mass is the shear strength, i.e. friction angle and cohesion, expressed as the maximum resistance to shearing stress. If external forces surpass this internal resistance, a failure occurs (Kezdi 1974). Landslides are commonly the results of sliding due to shear stress. A decrease in strength is often considered one of the causes of sliding. A weak layer is usually required to allow the development of a common slip surface.

Generally, the shear strength of a cohesive soil depends on soil structure, void ratio, and on the rate of shear deformation (Kezdi 1974). It has been found that the shear strength of a cohesive soil decreases with an increase in water content (Atkinson 1993; Scott 1963). Owing to natural consolidation by pressure, both the water content and void ratio decrease with depth, and therefore strength increases.

We had two objectives in carrying out this study. The first one was to determine the strength parameters of soil and rock samples obtained from a selected borehole in the Shiraidake landslide area and study of their behaviour. The triaxial test was carried out to analyse soil and soft rock samples whereas the unconfined compression test was applied in case of other rock samples. The second objective was to pursue the variation of the strength parameters with respect to the depth and the proximity to slip surface.

GEOLOGY OF THE AREA

The Early Miocene brackish non-marine strata and the Middle Miocene–Pliocene volcanic tuff and pyroclastic rocks are exposed in the Nagasaki Prefecture and they dip gently towards the northwest. The landslide area is formed of the Early Miocene Sasebo Group, which covers the Oligocene Kishima Group. The Sasebo Group is about 1,000 to 1,600 m thick. It is built up of eight formations, and the uppermost Kase Formation is made up of marine mudstone. Each of the other formations is composed of a single cyclothem that begins with a layer of marine or brackish facies and ends with a non-marine coal seam. The Sasebo Group is overlain

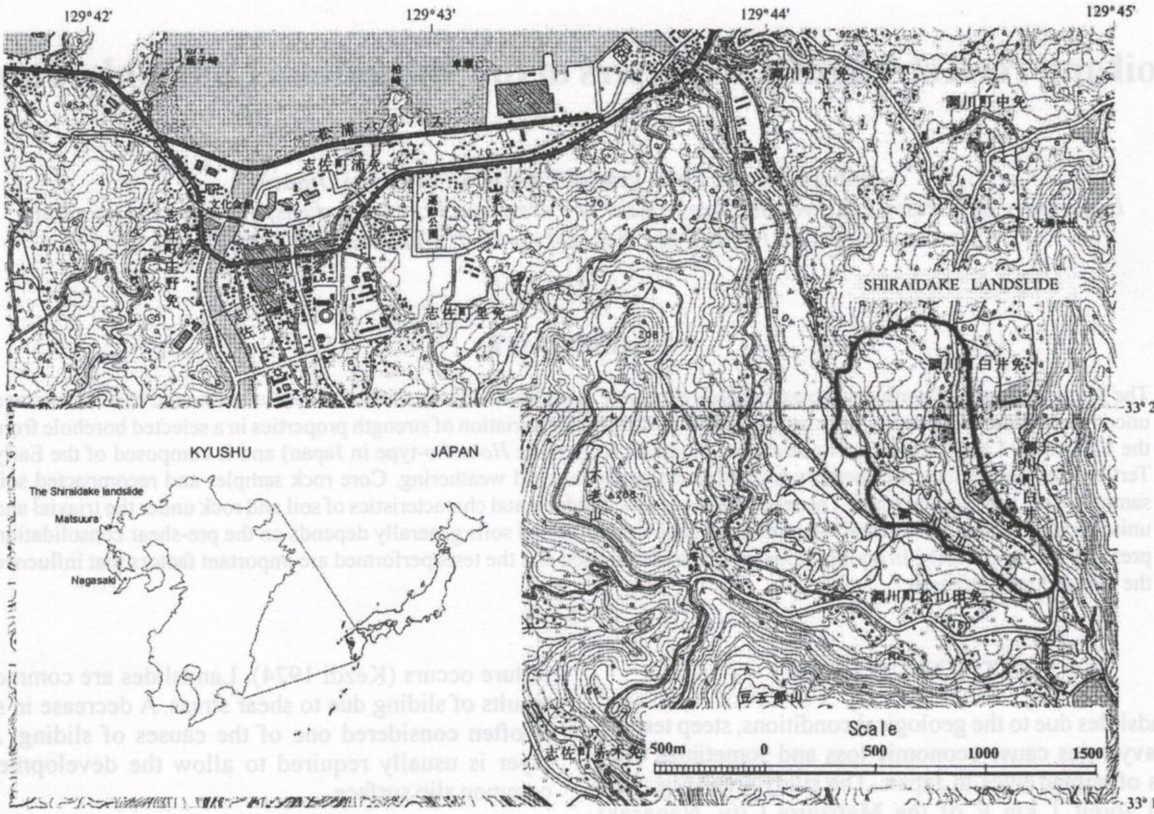

Fig. 1: Location of the Shiraidake Landslide in the northwestern Kyushu. The base map is from the Shisa and Emukae topographic sheets (1:25,000) of Japan.

by the Early to Middle Miocene Nojima Group and the Matsuura basalt flows. The latter are widely distributed in northwest Kyushu and occur repeatedly in the Late Miocene and Pliocene epochs.

The Quaternary strata are represented by the colluvial, delluvial, and alluvial deposits. They are usually horizontal and their depth rarely attains 100 m (Kimura et al. 1991).

SHIRAIDAKE LANDSLIDE

The Shiraidake Landslide is a moderately deep-seated translational slide, called the *Hokusho*-type. Generally, it is classified as a 'Tertiary landslide' in Japan. The extension of the affected area is approximately 1.3 km in length and 2 km in width. The landslide occurs on a gentle (5° to 6°) dip slope. The direction of movement is towards the west. Fig. 2 illustrates a cross-section of the Shiraidake Landslide with some retaining structures. The altitude in this block varies from 50 to 160 m.

The landslide was first noticed in 1945 and its investigation was carried out in 1952 and 1958, and the affected area was legally recognised as a landslide zone. Additional investigations were conducted in the 1990s, as the movement continued. Today the slope has been stabilised by effective retaining structures. The area is covered by vegetation and the gentle slope below the toe is covered by paddy fields.

There are usually complex factors that cause landslides. In the Shiraidake Landslide, the following causative factors are identified:

- Favourable geological structure and lithology (i.e. intercalation of coal seams between tuff layers), where the contact of strata can act as a slip plane,
- Interbedded impermeable and permeable rocks, and Quaternary gravel layer with the possibility of formation of perched aquifer system, and
- A gentle dip slope, which is typical for the occurrence of such landslides.

According to Ondrášik et al. (1996) who carried out the research in this area, the geological hazards depend not only on the very articulated and wrinkled topography and geology but also on the high-intensity rainfall in that region.

BOREHOLE H9-1

Drilling in the Shiraidake landslide area was done by Fujinagatiken Company. Samples from the Borehole H9-1 (Fig. 2) were selected for the laboratory analysis of the

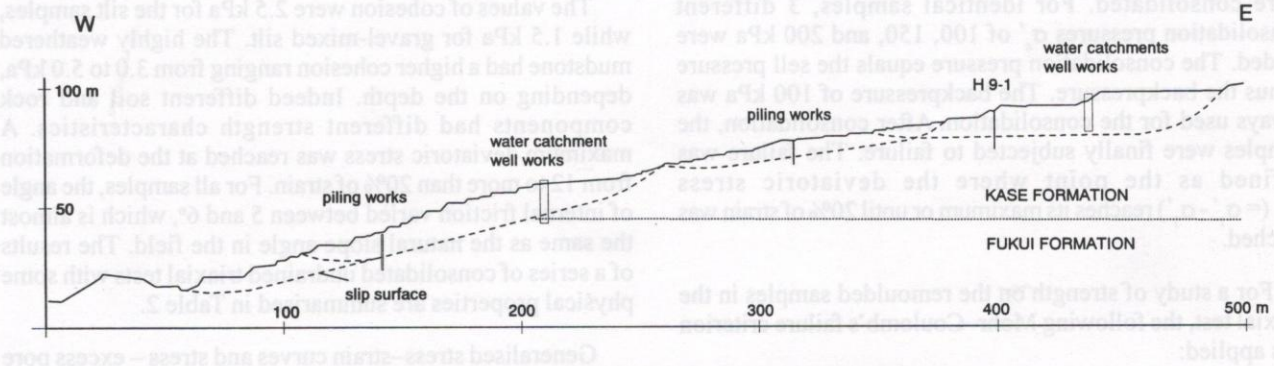

Fig. 2: Cross-section of the Shiraidake Landslide

strength properties. In this area, the landslide is underlain by the Tertiary sedimentary rocks of the Fukui Formation consisting mainly of sandstone, shale, mudstone, tuff conglomerate intercalated with coal seams, and the Kase Formation composed of sandstone, mudstone, shale, and gravel with thin coal seams and tuff layers. Both formations belong to the Sasebo Group. Near the summit, these rocks are overlain by the Matsuura type of basalt as the cap rock and the Quaternary deposits.

Lithology of the Borehole H9-1 and the depth of tested samples are given in Table 1. There are six lithological layers in the above borehole with the total depth of 15 m. Eight borehole samples from different layers were examined in the laboratory. The topsoil was excluded from the analysis. Below the topsoil, a zone of yellowish brown silt and gravel-mixed silt is observed up to the depth of 4.30 m. The lower part of the borehole is made up of dark grey mudstone and coarse- to medium-grained, yellowish brown sandstone. Two mudstone layers are presented in the borehole. The first one (from 4.30 to 10.20 m) is highly weathered and the second one (from 10.20 to 14.35 m) is slightly weathered or intact mudstone. Based on the boring data, the slip surface has been identified at a depth of about 10 m. In the dry season, the water table in this borehole is at a depth of about 4 m.

Table 1: Borehole log of H9-1 with sample numbers and corresponding depths

Soil/rock type	Layer depth (m)	Sample No	Sample depth (m)
Surface soil	0.0–0.35	-	0.00–0.35
Silt	0.35–0.70	1	0.35–0.70
Gravelly silt	0.70–4.30	2.1	0.70–3.00
		2.2	3.00–4.30
Strong weathered mudstone	4.30–10.20	3.1	4.30–6.00
		3.2	6.00–7.50
		3.3	7.50–10.20
Mudstone	10.20–14.35	4	10.20–14.35
Sandstone	14.35–15.00	5	14.35–15.00

TEST PROCEDURES

Values of the strength parameters can be determined using a variety of laboratory methods or in situ tests. Despite the different soil and rock samples, we attempted to evaluate their strength properties according to the sample depth and proximity to the slip surface.

In the present study, to determine the shear strength parameters of soft rock and soil samples (i.e. Sample Nos. 1, 2.1, 2.2, 3.1, 3.2, and 3.3) the triaxial test was carried out. For the other rock samples (i.e. Sample Nos. 4 and 5), shear strengths were estimated with the unconfined compression test. In addition, the results obtained from the standard penetration tests (Report 1997) were compared with the results from the laboratory tests.

The state of the soil was described by specific density determined in accordance with ASTM standards using the pycnometer method and by dry density determined by the paraffin method.

Triaxial test

The triaxial test is the most widely used laboratory method to determine the shear parameters, because it simulates the real stress–strain state in a soil or rock mass. A strain-controlled loading apparatus with strain rate of 0.05% per minute was used to perform consolidated undrained (CU) compression test with the pore pressure measurement.

The recompacted samples were used to determine the strength properties. Based on a specific dry density, material was compacted into a split mould of known dimensions from each of the five layers. The dimensions after extrusion from the split mould were 50 mm in diameter and approximately 100 mm in height.

The CU triaxial test was carried out on sets of 6 samples. The samples were first saturated in the triaxial cell, where a backpressure (Δu) of 5 kPa and a cell pressure (σ_c) of 8 kPa were used. Skempton's B value ($B = \Delta u/\Delta\sigma_c$) was always equal to or higher than 0.95. After saturation, the samples were consolidated. For identical samples, 3 different consolidation pressures σ_c' of 100, 150, and 200 kPa were loaded. The consolidation pressure equals the sell pressure minus the backpressure. The backpressure of 100 kPa was always used for the consolidation. After consolidation, the samples were finally subjected to failure. The failure was defined as the point where the deviatoric stress $\Delta\sigma$ ($=\sigma_1' - \sigma_3'$) reaches its maximum or until 20% of strain was reached.

For a study of strength on the remoulded samples in the triaxial test, the following Mohr–Coulomb's failure criterion was applied:

$$\sigma'_{1f} - \sigma'_{3f} = 2c\cos\phi + \left(\sigma'_{1f} + \sigma'_{3f}\right)\sin\phi \quad (1)$$

where σ'_{1f} is effective major principal stress at failure in kPa, σ'_{3f} is effective minor principal stress at failure in kPa, and ϕ is angle of internal friction.

The strength parameters (i.e. cohesion and angle of internal friction) were determined using the following expressions and graphically using a schematic diagram (Fig. 3).

$$\phi = \sin^{-1} m_i \quad (2)$$

$$c = \frac{f_i}{\sqrt{1+m_i}} \quad (3)$$

where m_i is inclination of the straight line, f_i is distance up to the intersection of the straight line with the vertical line, and c is cohesion in kPa.

The values of cohesion were 2.5 kPa for the silt samples, while 1.5 kPa for gravel-mixed silt. The highly weathered mudstone had a higher cohesion ranging from 3.0 to 5.0 kPa, depending on the depth. Indeed different soil and rock components had different strength characteristics. A maximum deviatoric stress was reached at the deformation from 12 to more than 20% of strain. For all samples, the angle of internal friction varied between 5 and 6°, which is almost the same as the natural slope angle in the field. The results of a series of consolidated undrained triaxial tests with some physical properties are summarised in Table 2.

Generalised stress–strain curves and stress – excess pore pressure curves under the triaxial compression test are illustrated in Fig. 4. The characteristics of the stress–strain and the pore pressure behaviour were practically identical

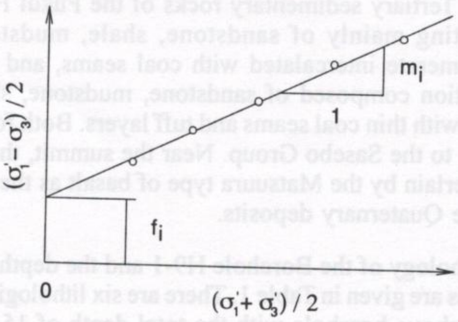

Fig. 3: Schematic diagram for the determination of cohesion and internal friction angle

Table 2: Results of the physical and strength properties obtained from the triaxial test

Sample No.	Depth (m)	Specific gravity	Dry density (g/cm³)	Consolidation pressure (kPa)	At failure: Deviator stress (kPa)	At failure: Strain (%)	Cohesion (kPa)	Angle of internal friction (°)
				100	15.9	15		
1	0.35–.70	2.58	1.67	150	23.3	20	2.5	5.2
				200	26.4	20		
				100	18.6	20		
2.1	0.70–.00	2.59	1.68	150	21.6	20	1.5	5.5
				200	29.6	15.5		
				100	14.2	13		
2.2	3.00–4.30	2.64	1.68	150	23.0	20	1.5	5.5
				200	25.6	19.5		
				100	25.7	20		
3.1	4.30–6.00	2.66	1.98	150	34.4	13.5	3.0	5.7
				200	36.9	14.5		
				100	32.8	12		
3.2	6.00–7.50	2.68	1.99	150	34.9	18	3.5	5.5
				200	40.9	14.5		
				100	28.7	20		
3.3	7.50–10.20	2.70	2.02	150	36.8	15	5.0	5.5
				200	43.7	17.5		

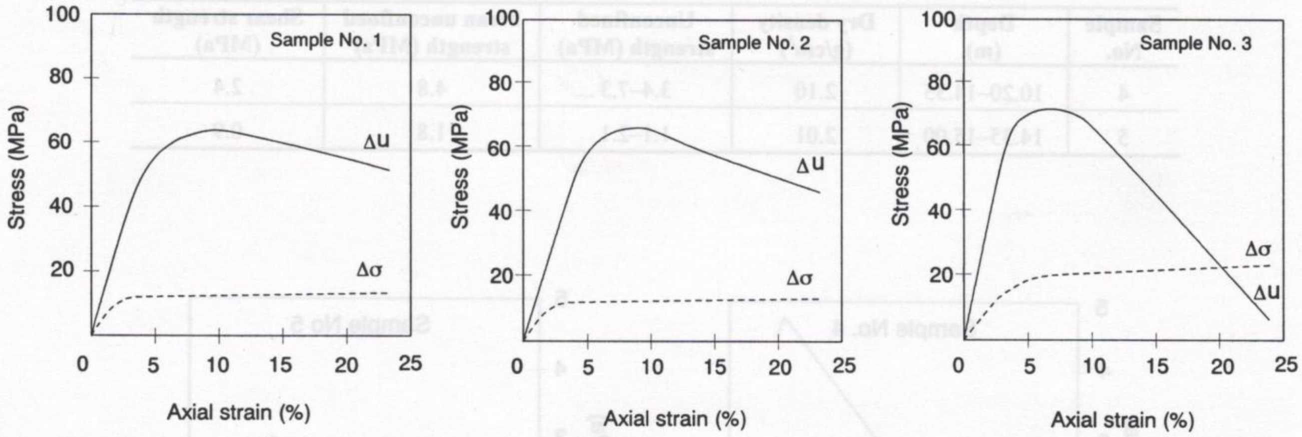

Fig. 4: Generalised stress–strain curves and stress – excess pore pressure curves for silt (Sample No. 1), gravel-mixed silt (Sample No. 2), and highly weathered mudstone (Sample No. 3)

for Sample Nos. 1 and 2. At first, the pore water pressure rapidly increased and at the strain of about 5 % reached a maximum, after which slowly decreased. The stress–strain diagram is a smooth curve, with increasing shear strains, the shear stress continuously increases. Sample No. 3 behaved similarly to Sample Nos. 1 and 2; the pore water pressures reached a maximum at the same strain of about 5%, but after which started to dramatically decreased. All samples showed a dilative response before and during the failure.

Almost all samples had a plastic type of failure with typical 'barrel-shape'; only some mudstones exhibited a brittle failure with a well-defined slip surface.

Very low values of the shear strength parameters can be attributed to the nature of the material tested, i.e. the remoulded samples and also due to a high degree of weathering in the case of mudstone samples. It is generally known that the weathering results in a significant reduction of the rock strength. The actual strength parameter values of the recompacted samples were considered of less importance and more emphasis was placed on their variation according to the depth. The results showed that the undrained behaviour of tested soils depended on the dry density and the pre-shear consolidation pressure.

Unconfined compression test

Another commonly used method of measuring the cohesive strength of soil or rock is the unconfined compression test. The test is quick and easy to perform. The unconfined compression test is similar to the triaxial test except that no lateral pressure is applied.

Cylindrical core samples, with a length-to-diameter ratio of 2, were tested by static compression. An axial load at a strain rate of 0.5% per minute was increased until the sample failed. A peak value of the axial stress was taken as the unconfined compressive strength. The shear strength was roughly assumed to be half of the unconfined compression strength (Rahn 1995). Simultaneously with the axial load, the displacement was also measured by a micrometer gauge. These data were used for drawing the stress–strain curves.

The unconfined compression test was carried out on the slightly weathered mudstone and sandstone samples. Because of the limited samples available, the test was repeated 12 times for the mudstone and only 4 times for the sandstone samples, and their mean values of the unconfined strength and the shear strength were calculated. The range of the unconfined strength for mudstone varied between 3.4 and 7.3 MPa, with a mean value of 4.8 MPa, while for sandstone the range was a little lower, from 1.1 to 2.1 MPa, with the mean value of 1.8 MPa (Table 3).

Both mudstone and sandstone samples failed by irregular brittle splitting. A typical pattern of the stress–strain curves in the unconfined compression for tested mudstone and sandstone is illustrated in Fig. 5.

The stress–strain plot of the slightly weathered mudstone shows feeble plastic behaviour at a very low stress level, then almost linear behaviour, after which it fails. Sand samples behave elastically at the beginning of the stress–strain curves, and then they become almost linear and finally fail.

THE STANDARD PENETRATION TEST AND A COMPARISON OF THE RESULTS

The number of blows (SPT-N blows) in the standard penetration test are scattered between 3 and 18, and the test was stopped when the number exceeded 50. The values obtained from the standard penetration test were similar to

Table 3: Results of the strength parameters obtained from the unconfined compression test

Sample No.	Depth (m)	Dry density (g/cm^3)	Unconfined strength (MPa)	Mean unconfined strength (MPa)	Shear strength (MPa)
4	10.20–14.35	2.10	3.4–7.3	4.8	2.4
5	14.35–15.00	2.01	1.1–2.1	1.8	0.9

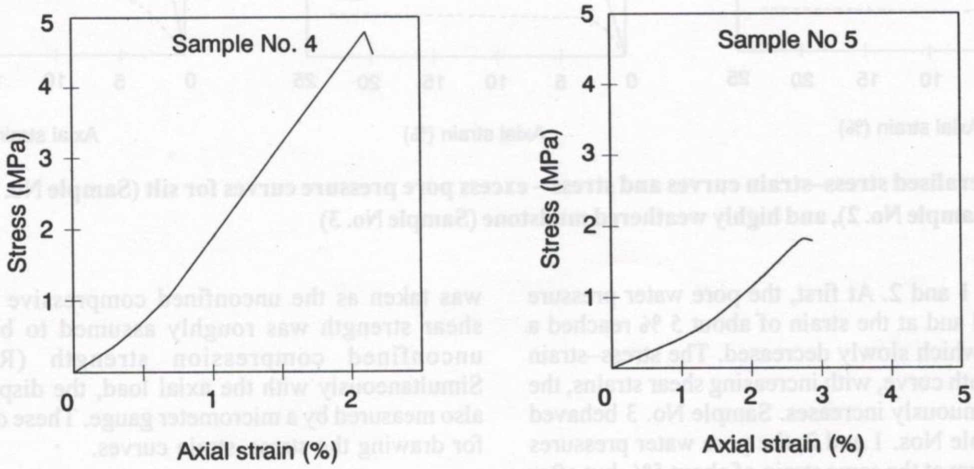

Fig. 5: Generalised stress–strain curves for tested mudstone (Sample No. 4) and sandstone (Sample No. 5)

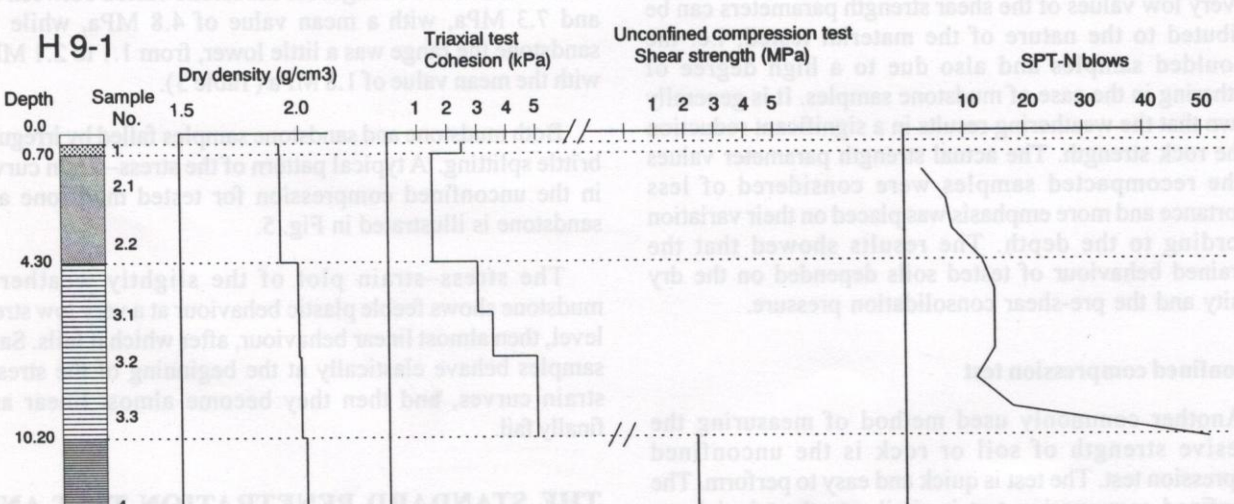

Fig. 6: lithological and geotechnical profile of the Borehole H9-1

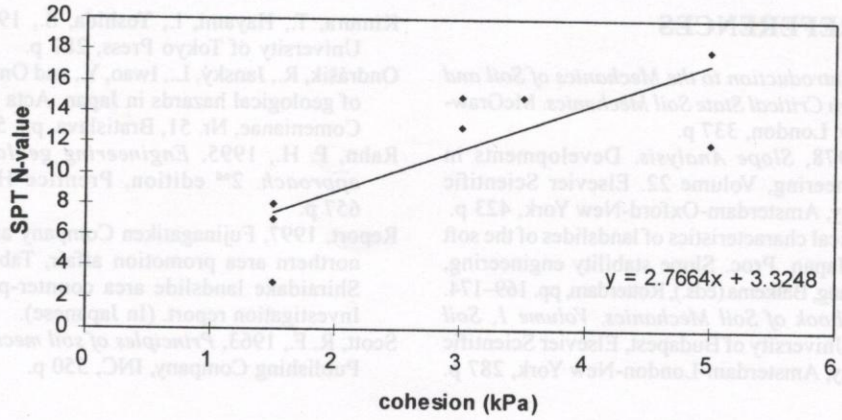

(a)

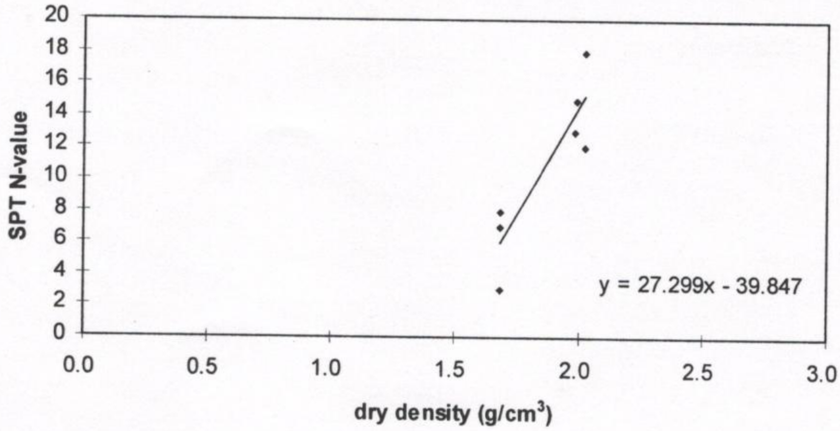

(b)

Fig. 7: a. Correlation between the standard penetration number of blows and cohesion; b. between the standard penetration number of blows and dry density

those from the triaxial and unconfined compression tests. It can be seen in Fig. 6 where dry density and cohesion are also displayed as a stair-step plot. Considering this, regression analyses between SPT-N blows and cohesion and also between SPT-N blows and dry density were carried out. The relationship is illustrated in Fig. 7a and 7b.

The regression analysis yielded a good correlation for the best-fit line with the following expressions:

$$N = 2.7664\, c' + 3.3248,\ \mathrm{r} = 0.79 \qquad (4)$$

$$N = 27.299\, \rho_d - 39.847,\ \mathrm{r} = 0.90 \qquad (5)$$

where N, c', r, and ρ_d are SPT-N blows, cohesion, regression coefficient, and dry density, respectively.

Both above relationships fall within the 95% of significance level.

CONCLUSIONS

The present study was carried out in an attempt to understand strength properties and their behaviour according to depth in the Shiraidake landslide area. A series of undrained triaxial tests with pore pressure measurements were conducted on saturated soil and soft rock samples and also the unconfined compression tests were conducted on rock samples obtained from the Borehole H9-1.

The results indicate that the undrained behaviour of tested soils depends on the pre-shear consolidation pressure and also on dry density. However, the strength does not appear to be a function of only these two factors. Other factors such as the loading path, fabric and grain arrangements, soil structure, and void ratio also influence the shear strength.

The significance of the standard penetration number of blows and cohesion, and between the standard penetration number of blows and dry density relationships was evaluated through the regression analysis and the results showed a strong correlation between the two parameters.

Low values of the strength parameters also indicate their dependency on the degree of weathering, type of the sample used, and the kind of test performed.

REFERENCES

Atkinson, J., 1993, *An Introduction to the Mechanics of Soil and Foundation: Through Critical State Soil Mechanics.* McGraw-Hill Book Company, London, 337 p.

Chowdhury, R. N., 1978, *Slope Analysis.* Developments in Geotechnical Engineering, Volume 22. Elsevier Scientific Publishing Company, Amsterdam-Oxford-New York, 423 p.

Fujita, T., 1999, Geological characteristics of landslides of the soft rock type, Central Japan. Proc. Slope stability engineering, Yagi, Yamagami & Jiang, Balkema (eds.), Rotterdam, pp. 169–174.

Kezdi, A., 1974, *Handbook of Soil Mechanics, Volume 1, Soil Physics.* Technical University of Budapest, Elsevier Scientific Publishing Company, Amsterdam-London-New York, 287 p.

Kimura, T., Hayami, I., Yoshida, S., 1991, *Geology of Japan.* University of Tokyo Press, 287 p.

Ondrášik, R., Janský, L., Iwao, Y., and Omura, H., 1996, Research of geological hazards in Japan. Acta Geologica Universitatis Comenianae, Nr. 51, Bratislava, pp. 5–15.

Rahn, P. H., 1995, *Engineering geology: an environmental approach.* 2nd edition, Prentice Hall PRT, New Jersey, 657 p.

Report, 1997, Fujinagatiken Company and Nagasaki prefecture, northern area promotion affair, Tabira public work office, Shiraidake landslide area counter-plan construction work. Investigation report. (In Japanese).

Scott, R. F., 1963, *Principles of soil mechanics.* Addison-Wesley Publishing Company, INC, 550 p.